Collision Free Dynamic Stability of Formations Using Projection Based Estimators

Vinod P. Gehlot and Mark J. Balas
Mechanical Engineering Department
Texas A&M University, College Station, Texas 77843
email: {vinodgehlot, mbalas}@tamu.edu

Saptarshi Bandyopadhyay, Marco B. Quadrelli, and David S. Bayard
Jet Propulsion Laboratory
California Institute of Technology, Pasadena, California 91125
email: {saptarshi.bandyopadhyay, marco.b.quadrelli, david.s.bayard}@jpl.nasa.gov

***Abstract*— Transient instability is a phenomenon where inter-agent collisions can occur in dynamically stable formations of autonomous agents. Therefore, the necessity to manage and mitigate transient instabilities is essential for successfully deploying formation structures. This paper develops a novel control architecture that augments the baseline formation maintenance controller to mitigate transient instabilities. At its heart, the proposed architecture consists of a projection operator based estimator disguised as a reference model that generates collision-free trajectories for the agents to follow. This paper's main theoretical result shows that the proposed control architecture can simultaneously mitigate transient instabilities and guarantee asymptotic convergence of the formation dynamics. Also, an illustrative example demonstrates the theoretical developments presented in this paper.**

I. INTRODUCTION

A multi-agent system is an organization of several individual dynamic entities that collaboratively accomplish a common objective that would be impossible or very difficult to achieve with a sole individual. Formations are multi-agent systems where their entities interact to achieve a desired geometric shape or configuration, and they are particularly useful in large scale sensing and mapping applications. Localization, the process of determining a location in space, can be an incredibly tricky problem to solve for agents operating in unknown environments or in deep space applications. Therefore, the use of absolute position measurements, by the agents, for the coordination of a formation can be too restrictive. On the other hand, relative position measurements made by onboard sensors, such as radar or lidar, are a more practical approach to formation maintenance than absolute coordinates. A typical control approach to formation maintenance is relative error feedback, which is the feedback of the difference between the desired relative separation and the measured relative positions, applied to every agent. If the closed-loop dynamics with relative error feedback are asymptotically—or better exponentially—stable, all the agents will satisfy their desired relative separation, and the formation achieves its geometric centrifugation. We discuss the relative feedback approach to formations and their exponential stability in our previous work [1]; other notable references include [2], and [3].

By itself, asymptotic stability of relative error dynamics alone is not enough for the safe operation of formations. In highly dynamic formation reconfigurations and tightly packed multi-agent systems, inter-agent collisions can occur due to the transient dynamics of an otherwise asymptotically stable relative error trajectory; we define this phenomenon as *transient instability*. A formation is said to be *transient stable* if 1) its relative error dynamics are stable in the sense of Lyapunov, and 2) the relative error dynamics result in the collision-free evolution of the formation. Peppard in [4] introduced and derived the necessary conditions for "string stability" in serial chain vehicle platoons. Although string stability guarantees asymptotic stability, it does not imply collision-free relative dynamics. In [5], the authors develop a novel control approach to formation construction and reconfiguration and show that it is possible to satisfy collision-free exponential stability in two-agent systems. Recently, in [6], the authors develop a unique control approach to satisfying transient stability using Control Barrier Functions (CBF). Here, the simultaneous problems of exponential stability and collision-avoidance are posed as a Quadratic Program (QP) and solved continuously; it is a centralized control approach. In the comprehensive survey of multi-agent algorithms [7], the coordination and control algorithms fall into two distinct categories: predictive and reactive.

Furthermore, with regards to formation maintenance, neither predictive nor reactive algorithms can satisfy transient stability. In the literature, fundamental theoretical results on transient stability tend to be either too restrictive — like particular formation types, cardinality, and configurations — or too centralized. Therefore, it is imperative to address the issues of transient instabilities in more general and decentralized formation geometries. This paper introduces a novel decentralized control approach to mitigating transient instabilities in arbitrary formations using projection-based estimator dynamics and presents the associated theoretical underpinnings, including stability results, for the proposed architecture. This paper has two main contributions: first, the transient stable control approach shown in Fig. 1, which consists of the relative error feedback controller and the combined projection-based collision-free trajectory generator and the tracking controller, and second, the main theoretical result, which provides the proof for the collision-free asymptotic stability of the inter-agent relative error dynamics.

We begin with a qualitative discussion of the control architecture in Fig. 2 and claim that it provides transient stability in arbitrary formations; later in Section IV, we will present our main result to substantiate this claim. We assume that every agent's dynamics in the formation are identical and linear, and available to every agent, through some output matrix, is the average of the relative error measurement of all its neighbors. Also, we assume that the control information from the neighboring agents are made available to every agent in the formation. The agents use the output relative error measurements and communicated control information to accomplish formation maintenance via an output feedback control law; this forms the *agent + baseline formation controller* in Fig. 1. As discussed earlier, although the formation maintenance controller will drive the agents to their respective positions in space asymptotically, it alone cannot provide transient stability. The *collision free trajectory estimator + tracking controller*, in Fig. 1, augments the closed-loop agent dynamics and mitigates any transient behavior that may cause inter-agent collisions. Unmodified, the *relative state estimator* with stable error dynamics will precisely track the actual relative error. The projection operator modifies the estimated relative error dynamics so that the estimated relative trajectory will never exceed the safe transient bounds. Finally, the tracking controller drives the actual relative state vector, of the agent, to the estimated state vector and thwarting any inter-agent collisions that might occur during transients.

In this paper, we present and discuss our results in four sections: Section II establishes the formation dynamics that arise from the interaction of linear agent dynamics and describes the stability benefits of inter-agent communication, Section III introduces the constraints for collision-free relative error dynamics, the projection operator and the estimator dynamics, and few preliminary results central to proving projection-based dynamics. Here, we also give the precise definition of transient stable formation dynamics. In Section IV, we present our main theoretical result on transient stability, and finally, in Section V we use an illustrative example to demonstrate the application of the theoretical results and the control structure shown in Fig. 1. Before moving onto Section II, we briefly introduce the notation used in this paper to describe the theoretical results.

A. Formation Dynamics Notation

- **Spaces**: The state vector of every individual agent is an n-dimensional vector space $\mathbf{X} \equiv \mathbb{R}^n$. The agent's inputs and outputs evolve in the m-dimensional input space $\mathbf{U} \equiv \mathbb{R}^m$ and the p-dimensional output space $\mathbf{Y} \equiv \mathbb{R}^p$, respectively.

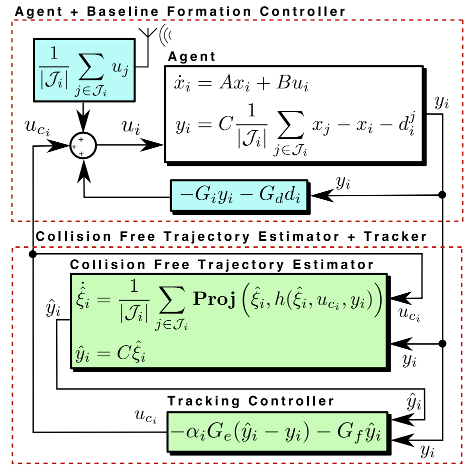

Fig. 1. An individual agent's control structure for mitigating transient instabilities; all the agents in the formation, except the leader, are equipped with the same control architecture.

- **Indices**: $\mathscr{I} \equiv \{1, 2, \ldots, N\}$ is the index set of all the agents in the formation. The index variable $i \in \mathscr{I}$, used exclusively as a subscript on vectors, refers to the i^{th} agent in the formation. The subset $\mathscr{J}_i \subset \mathscr{I} \setminus i$, is the index set of all the neighbors of the i^{th} agent. The index variable $j \in \mathscr{J}_i$, used mostly as a superscript on vectors, refers to the j^{th} neighbor of the i^{th} agent.
- **Vectors**: Every vector — except those representing collective behavior — have subscripts i or j. For example, $x_i \in \mathbf{X}$ is the state vector of the i^{th} agent. A vector can also have a superscript j, along with the subscript i, to indicate a vector directed from the i^{th} agent to the j^{th} agent. For example, the vector d_i^j is the constraint vector originating at the i^{th} agent and terminating at the j^{th} neighbor.

II. FORMATION DYNAMICS

In this section, we establish the dynamics of the formation, beginning with the agent dynamics. Following this, we introduce the relative error vector, the formation control policy assuming inter-agent communication, and the overall relative error dynamics for the entire formation.

A. Agent Dynamics

The dynamics of every agent i in the formation is the Linear-Time-Invariant (LTI) system of the from

$$\dot{x}_i = Ax_i + Bu_i \tag{1a}$$

$$y_i = Cx_i. \tag{1b}$$

Here, $x_i \in \mathbf{X}$ is the state vector of the agent, $u_i \in \mathbf{U}$ the input vector, and $y_i \in \mathbf{Y}$ the output vector. The matrix tuple (A, B, C) are appropriately sized constant matrices describing the linear dynamics of the agent.

B. Relative Error Vector

Relative error vector and its feedback is the primary mechanism for formation's geometric configuration. For all the $|\mathscr{J}_i|$ neighbors of the agent i, the relative error vector is the average vector

$$\xi_i = \frac{1}{|\mathscr{J}_i|}\sum_{j\in\mathscr{J}_i}\xi_i^j. \tag{2}$$

Here,

$$\xi_i^j = x_j - x_i - d_i^j \tag{3}$$

is the individual relative error vectors for each neighbor $j \in \mathscr{J}_i$. The vector $d_i^j \in \mathbf{X}$ is the constraint vector and it evolves according to the *command generator dynamical system*

$$\dot{\eta}_i^j = F\eta_i^j \quad ; \eta_i^j(0) \in X \tag{4a}$$

$$d_i^j = \Theta\eta_i^j \quad ; d_i^j \in \ker(A). \tag{4b}$$

In (4), the matrix F describes the dynamics of the vector η_i^j. The matrix $\Theta \ni \Theta^2 = \Theta$, is a projection of the command generator vector η_i^j on to the null space of the agent dynamic matrix A; it maps the vector η_i^j to the output d_i^j. Therefore, the constraint vector d_i^j resides in the $\ker(A)$. Although not necessary, this assumption allows for the agents to maintain the separation between their neighbors without the use of a constant control effort. Fig. 2 and Fig. 3 show the relative error vector for single and multiple neighbors, respectively. In Fig. 3, the vector $\tilde{\xi}_i^j$ is the scaled vector $\xi_i^j/|\mathscr{J}_i|$, and the same follows for $\tilde{\xi}_i^k$, $\tilde{\xi}_i^l$, and $\tilde{\xi}_i^m$.

Remark 1: The relative error vector ξ_i^j, as defined in (3), is the difference between the desired and current states of the agent, and it is markedly different from the usual position or velocity based definition of relative error in 2D or 3D Euclidean space; it allows for very general constraint definitions.

C. Derivation of the Formation Control Policy Based on Agent-to-Agent Communication

Let q_i^j be a vector defined by $q_i^j \equiv x_j - x_i$. Its time derivative is

$$\begin{aligned} \dot{q}_i^j &= \dot{x}_j - \dot{x}_i = Aq_i^j + Bu_i^j, \text{ and} \\ y_i^j &= Cq_i^j, \end{aligned} \tag{5}$$

where, $u_i^j = u_j - u_i$. In a formation, the maintenance of its geometry occurs by regulating all of its agents' relative error vector ξ_i, which is the same problem as all of the q_i^j tracking all the constraint vectors d_i^j. The principle of ideal trajectories in [8] solves the problem of tracking using output feedback. Here, we use the principle of ideal trajectories to determine the formation control law for the input u_i. Let q_i^{*j} be the ideal trajectory of q_i^j, along with the ideal input u_i^{*j}, that evolves according to the ideal dynamics

$$\dot{q}_i^{*j} = Aq_i^{*j} + Bu_i^{*j} \tag{6a}$$

$$y_i^{*j} = Cq^{*j} = Cd_i^j. \tag{6b}$$

The coordinate transformation

$$\begin{pmatrix} q_i^{*j} \\ u_i^{*j} \end{pmatrix} = \begin{pmatrix} S_{11} & S_{12} \\ G_d & S_{22} \end{pmatrix}\begin{pmatrix} d_i^j \\ 0 \end{pmatrix} \tag{7}$$

defines the relationship between the ideal trajectory dynamics (6) and the dynamics of the constraint vector d_i^j in (4). From (6), (7), $q_i^{*j} = S_{11}d_i^j$, $u_i^{*j} = G_d d_i^j$, and by taking the time derivative of q_i^{*j}, we arrive at the matching conditions:

$$(AS_{11} + BG_d)\Theta = S_{11}\Theta F \quad \text{and} \tag{8a}$$

$$S_{11} = I_{n\times n}. \tag{8b}$$

The error dynamics between the ideal trajectory in (6) and the dynamics of the vector q_i^j in (5) is the controllable and observable system

$$\Delta\dot{q}_i^j = A\Delta q_i^j + B\Delta u_i^j \tag{9a}$$

$$\Delta y_i^j = C\Delta q_i^j. \tag{9b}$$

Here, $\Delta q_i^j \equiv q_i^j - q_i^{*j}$, $\Delta u_i^j \equiv u_i^j - u_i^{*j}$, and $\Delta y_i^j = C\Delta q_i^j = C\xi_i^j$. Provided the error system (9) meets the conditions [9] for output feedback stabilization, there exists an appropriately sized gain matrix, G_i, so that the control law,

$$\Delta u_i^j = G_i C\Delta q_i^j \tag{10}$$

results in the close-loop error system

$$\Delta\dot{q}_i^j = (A + BG_iC)\Delta q_i^j \tag{11a}$$

that is exponentially stable. Moreover,

$$\Delta q_i^j \to 0 \Rightarrow \quad \Delta y_i^j = C\Delta q_i^j = C\xi_i^j \to 0 \text{ as } t \to \infty. \tag{12}$$

Taking the time derivative of (3) yields the relative error dynamics

$$\dot{\xi}_i^j = \dot{x}_j - \dot{x}_i - \dot{d}_i^j \tag{13a}$$

$$= A(x_j - x_i) + B(u_j - u_i) - \Theta F\eta_i^j \tag{13b}$$

The control law in (10) determines the control policy for the i^{th} agent:

$$\Delta u_i^j = u_i^j - u_i^{*j} = G_i C\xi_i^j. \text{ Also, } u_i^j = u_i - u_j \;\&\; u_i^{*j} = G_d d_i^j$$

$$\Rightarrow u_i = \begin{cases} u_j - G_iC\xi_i^j - G_d d_i^j & \text{if } |\mathscr{J}_i| \neq 0 \\ 0 & \text{otherwise.} \end{cases} \tag{14}$$

Substituting (14) into (13), results in

$$\dot{\xi}_i^j = (A + BG_iC)\xi_i^j + (BG_d\Theta - \Theta F)\eta_i^j. \tag{15}$$

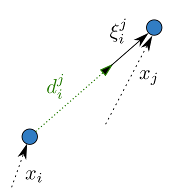

Fig. 2. Relative error vector for a single neighbor.

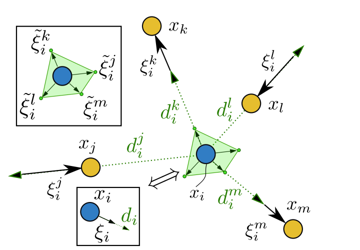

Fig. 3. Relative error vector for multiple neighbors; the top figure shows the $1/4$ scaled individual relative error vectors for the four agents; the bottom figure is the average relative error vector.

From the matching conditions in (8),

$$BG_d\Theta - \Theta F = -A\Theta. \tag{16}$$

Therefore,

$$\dot{\xi}_i^j = (A + BG_iC)\xi_i^j - A\Theta\eta_i^j. \tag{17a}$$

But, $A\Theta\eta_i^j = Ad_i^j$, and since, by assumption, $d_i^j \in \ker(A)$, $Ad_i^j = 0$. Hence, the relative error dynamics of the i^{th} with respect to the j^{th} agent, reduces to

$$\dot{\xi}_i^j = (A + BG_iC)\xi_i^j. \tag{18}$$

For every j^{th} neighbor of i, (18) is the relative error dynamics, provided the control policy is (14). The control policy for all the neighbors is the weighted linear combination of the u_i^js for all the neighbors:

$$u_i = \begin{cases} \frac{1}{|\mathscr{J}_i|}\sum_{j\in\mathscr{J}_i}\left(u_j - G_iC\xi_i^j - G_d d_i^j - u_{c_i}\right) & \text{if } |\mathscr{J}_i| \neq 0 \\ 0 & \text{otherwise.} \end{cases} \tag{19}$$

Here, transient stability — i.e. collision free — requirements are met with the additional control input vector u_{c_i} (discussed later). Taking the time derivative of the combined relative error vector in (2), and substituting for u_i from (14), we have

$$\dot{\xi}_i = (A + BG_iC)\xi_i + Bu_{c_i}. \tag{20}$$

Let $\xi = (\xi_1, \ldots, \xi_N)^T$ be the combined relative error vector for all the agents in the formation, then the relative error dynamics for the entire formation has the form

$$\begin{pmatrix} \dot{\xi}_1 \\ \dot{\xi}_2 \\ \vdots \\ \dot{\xi}_N \end{pmatrix} = \underbrace{\begin{pmatrix} A+BG_1C & 0 & \cdots & 0 \\ 0 & A+BG_2C & \cdots & 0 \\ \vdots & & \ddots & \\ 0 & 0 & \cdots & A+BG_NC \end{pmatrix}}_{=\bar{\mathbf{A}}} \begin{pmatrix} \xi_1 \\ \xi_2 \\ \vdots \\ \xi_N \end{pmatrix}$$
$$\underbrace{\begin{pmatrix} B & 0 & \cdots & 0 \\ 0 & B & \cdots & 0 \\ \vdots & & \ddots & \\ 0 & 0 & \cdots & B \end{pmatrix}}_{=\bar{\mathbf{B}}} \underbrace{\begin{pmatrix} u_{c_1} \\ u_{c_2} \\ \vdots \\ u_{c_N} \end{pmatrix}}_{=u_c}, \tag{21}$$

or compactly as

$$\dot{\xi} = \bar{\mathbf{A}}\xi + \bar{\mathbf{B}}u_c. \tag{22}$$

Figure (4) illustrates the interaction and communication topology between some agent i and its neighbors in some arbitrary formation. Here, the agent i is interacting — taking control action based on relative error — with its neighbors $\{4, 12, 7, 9\}$, while receiving control information $\{u_4, u_{12}, u_7, u_9\}$ from its neighbors to determine the formation maintenance control policy (u_j) in (19).

Remark 2: In the control policy in (19), the availability of the control information u_j, via communication, plays a vital role in the stability of the formation structure; it reduces the drift vector field, $\bar{\mathbf{A}}\xi$, of the relative error dynamics to a diagonal matrix, thereby, making the assessment of stability straight forward.

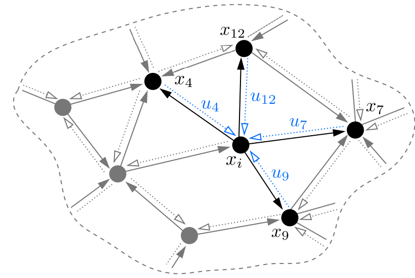

Fig. 4. Interaction and communication topology; for each interaction with a neighbor, the agent expects to receive its neighbor's control vector information.

Remark 3: Inter-agent communication has another remarkable upshot on the overall stability of a formation; it eliminates the interaction network's effect on the relative error dynamics, resulting in the diagonal formation matrix shown in (21). Without inter-agent communication, the spectrum of the Laplacian matrix of the interaction graph would scale the individual gain matrices, G_i, modifying the relative error vector's dynamic behavior [1]. Hence, inter-agent communication provides for consistent dynamic behavior for all agents regardless of their interaction topology.

Theorem 2.1 (Exponential Stability of Formation): The combined relative error trajectory, $\xi(t)$, of a formation is exponentially stable under the control policy in (19), if for every agent $i \in \mathscr{I}$, the closed-loop matrix

$$A + BG_iC, \tag{23}$$

is Hurwitz. Provided, for every agent $i \ni |\mathscr{J}_i| \neq 0$,

Proof: From (21), it is clear that the matrix $\bar{\mathbf{A}}$ is in diagonal form under the control policy u_i. And hence, the spectrum $\rho(\bar{A})$ is the set

$$\rho(\bar{A}) = \{\rho(A + BG_1C), \ldots, \rho(A + BG_NC)\}. \tag{24}$$

Therefore, the trajectory $\xi(t)$ is exponentially stable, provided, every closed-loop matrix $A + BG_iC$ is Hurwitz. ■

III. Constraints, Transient Stability, and Projection Based Stable Trajectory Estimators

Although Theorem 2.1 shows that the formation is exponentially stable, we know that it does not guarantee collision-free formation evolution. Therefore, in this section, we will develop the relative error based constraint for transient stable formation dynamics, define transient stability precisely, introduce the projection operator, and develop the projection-based estimator for generating collision-free reference trajectories.

A. Collision Free Relative Error Vector Constraints

The convex set Φ_i^j, defined by

$$\Phi_i^j = \left\{\hat{\xi}_i^j : (\hat{\xi}_i^j)^T\hat{\xi}_i^j - \left(1 - \alpha_i^j\right)^2 (d_i^j)^T(d_i^j) \leq 0\right\}, \tag{25}$$

describes the allowable region for the estimated relative error trajectories to evolve collision-free. Here, $0 < \alpha_i^j < 1$ is a positive constant used to specify the safety zone margin around an agent i concerning its neighbor j. Voronoi cell-based constraints developed in [10], for the collision avoidance of dynamic agents, inspired the definition of Φ_i^j. Though the two are not equivalent. The hard constraint that the relative error trajectory cannot violate is the positive scalar function

$$\tilde{\phi}_i^j = (1-\alpha_i^j)^2 (d_i^j)^T d_i^j. \tag{26}$$

For some scalar $\varepsilon > 0$, another positive scalar function

$$\bar{\phi}_i^j = \frac{(1-\alpha_i^j)^2 (d_i^j)^T d_i^j}{1+\varepsilon}, \tag{27}$$

defines the soft constraint boundary. The relative error vector is temporarily allowed to violate this constraint, and we will see later that it informs the projection operator to start modifying the estimated relative error trajectory. The convex set enclosed within the soft constraint boundary is

$$\bar{\Phi}_i^j = \left\{ \xi_i^j : (\xi_i^j)^T \xi_i^j - \frac{\left(1-\alpha_i^j\right)^2 (d_i^j)^T (d_i^j)}{1+\varepsilon} \leq 0 \right\}, \tag{28}$$

and we can use the parameter ε to determine the extent of the annulus between Φ_i^j and $\bar{\Phi}_i^j$. Fig. 5 uses an agent with two neighbors to illustrate the constraints discussed thus far. Finally, we have the precise definition of transient stablity in formations:

Definition 1 (Transient Stability): A formation of autonomous agents, with the dynamics defined by (1), is *transient stable* if, for every agent $i \in \mathscr{I}$, the relative error trajectory ξ_i evolves so that

$$\|\xi_i\|^2 \leq \sum_{j \in |\mathscr{J}_i|} (\xi_i^j)^T (\xi_i^j) \leq \sum_{j \in |\mathscr{J}_i|} \tilde{\phi}_i^j, \tag{29}$$

and $\|\xi_i(t)\| \to 0$, as $t \to \infty$.

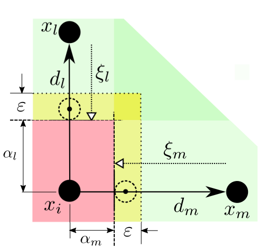

Fig. 5. Interaction constraints for an agent with two neighbors; the area in yellow is the soft boundary; the green area is the convex set $\bar{\Phi}_i^l + \bar{\Phi}_i^m$; the green and the yellow area, added together, represents the convex constraint set $\Phi_i^l + \Phi_i^m$; the relative error vector ξ_i is allowed to evolve within $\Phi_i^l + \Phi_i^m$.

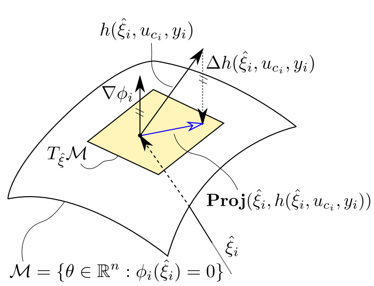

Fig. 6. Projection Dynamics; Here, the vector Δh is parallel to the constraint gradient $\nabla \phi_i$; the projection operator subtracts Δh from the vector field $h(\hat{\xi}_i, u_{c_i}, y_i)$.

B. Projection Operator Based Relative Trajectory Estimator

The projection operator has its origins in numerical solutions to constrained optimization problems. According to [11], Kreisselmeier and Narendra [12] introduced the projection operator as a mechanism to constrain time-varying parameters in adaptive systems. Since then, it has been hugely popular in several adaptive control algorithms [13][14][11] mainly due to its guarantee to heed its trajectory to the prescribed bounds while being Lipschitz continuous in operation. Consider an arbitrary nonlinear dynamical system with the differential equation $\dot{x} = f(x)$, and suppose that there is a limit on its evolution prescribed by the scalar convex constraint function $\phi(x) = 0$. The projection-based dynamics for $x(t)$ is the dynamical system

$$\begin{aligned} \dot{x} &= \mathbf{Proj}\,(x, f(x)) \\ &= \begin{cases} \left(I - \frac{\nabla\phi \nabla\phi^T}{\|\nabla\phi\|^2}\right) f(x) & \text{, if } \phi(x) > 0 \wedge f(x)^T \nabla\phi(x) > 0 \\ f(x) & \text{, otherwise,} \end{cases} \end{aligned} \tag{30}$$

and according to the Lemma 11.4 in [11], the trajectory will remain within the convex set defined by the boundary $\phi(x) = 0$.

Borrowing from this example, we create a projection-based estimator that generates collision-free relative error trajectories. The estimator, in this case, will be the reference model for the agent to follow. Let

$$\begin{aligned} \dot{\hat{\xi}}_i^j &= (A + BG_iC)\hat{\xi}_i^j + Bu_{c_i} + LC(\hat{\xi}_i^j - \xi_i^j) \\ \hat{y}_i^j &= C\hat{\xi}_i^j \end{aligned} \tag{31}$$

be the unmodified Luenberger estimator for the relative error trajectory for the j^{th} neighbor of agent i. The error dynamics for this estimator is

$$\dot{e}_i^j = (A + BG_iC + LC)e_i^j, \tag{32}$$

where $e_i^j = \hat{\xi}_i^j - \xi_i^j$. If we choose L such that the closed-loop matrix $A + BG_iC + LC$ is Hurwitz, then the estimator error dynamics will be exponentially stable, and the estimated relative error will converge to the actual relative error. From (27), we establish the convex constraint function

$$\phi_i^j = \phi(\xi_i^j) = \frac{(1+\varepsilon)\|\xi_i^j\|^2 - \|\bar{\phi}_i^j\|^2}{\varepsilon\|\bar{\phi}_i^j\|^2} \tag{33}$$

and enclose the estimator within the projection operator:

$$\begin{aligned} \dot{\hat{\xi}}_i^j &= \mathbf{Proj}(\hat{\xi}_i^j, h(\hat{\xi}_i^j, u_{c_i}, y_i^j)) \\ &= \begin{cases} \left(I - \frac{\nabla\phi_i^j (\nabla\phi_i^j)^T}{\|\nabla\phi_i^j\|^2}\right) h & \text{, if } \phi_i^j > 0 \wedge h^T \nabla\phi_i^j > 0 \\ h & \text{, otherwise,} \end{cases} \end{aligned} \tag{34}$$

where $h(\hat{\xi}_i^j, u_{c_i}, y_i^j) = (A + BG_iC)\hat{\xi}_i^j + Bu_{c_i} + LC(\hat{\xi}_i^j - \xi_i^j)$. According to Lemma 11.4 in [11], we know that the estimated relative error state will never exceed the boundary, $\tilde{\phi}_i^j$, provided the initial condition for the estimator state is within the set $\bar{\Phi}_i^j$. By subtracting from the estimator vector field, the normal component to the constraint manifold, the projection operator restricts the estimated relative error trajectory to the set Φ_i^j (see Fig. 6). However, is the error dynamics for the projection-based estimator stable? At this point, it is hard to say since the projection operator induces nonlinear dynamics into the otherwise linear relative error estimator dynamics. As part of the main result of transient stability, we will prove the projection-based estimator dynamics' exponential stability in Section IV, and in doing so, we will need the following important lemma on the projection operator:

Lemma 3.1 (Projection Inequality): Let $\hat{\xi}_i^{j*}$ be point in the interior of the convex set Φ_i^j, and let $\Gamma > 0$ be some positive definite and symmetric matrix, then for any other $\hat{\xi}_i^j(t) \in \Phi_i^j$,

$$(\hat{\xi}_i^j - \hat{\xi}_i^{j*})^T \left(\Gamma^{-1}\mathbf{Proj}\left(\hat{\xi}_i^j, \Gamma h(\hat{\xi}_i^j, u_{c_i}, y_i^j)\right) - h\right) \leq 0. \quad (35)$$

Proof: Refer to pg. 332 in [11]. ■

IV. Main Result: Control Architecture for Transient Stable Formations

The following is the main result of this paper. It shows the necessary condition under which the proposed control structure in Fig. 1 is adequate to mitigate transient instabilities in general N-Dimensional formations.

Theorem 4.1 (Transient Stability for Arbitrary Formations): An arbitrary N-agent formation is transient stable under the control policy

$$u_i = \underbrace{-\beta_i G_e C \frac{1}{|J_i|}\sum_{j\in\mathscr{J}_i}(\hat{\xi}_i^j - \xi_i^j) - G_f C \frac{1}{|J_i|}\sum_{j\in\mathscr{J}_i}\hat{\xi}_i^j}_{=u_{c_i}} + \frac{1}{|J_i|}\sum_{j\in\mathscr{J}_i}\left(u_j - G_i C\xi_i^j - G_d d_i^j\right). \quad (36)$$

Provided, the pair (A,B) and (A,C), of the agent dynamics in (1), are controllable and observable, Almost Strictly Dissipative (ASD)[15], and

$$\beta_i = \frac{\sqrt{\lambda_{\min}(Q_e)}\sqrt{\lambda_{\min}(Q_\xi)}}{\|G_e\|\,\|C\|^2} - \frac{\|G_f\|}{\|G_e\|} \quad (37)$$

for some positive definite matrices Q_e and Q_ξ.

Proof: From (18), and the control policy in (36), the overall closed-loop relative error dynamics for the i^{th} agent reduces to

$$\begin{aligned}\dot{\xi}_i &= (A + BG_iC)\xi_i + Bu_{c_i}\\ &= \bar{A}_i\xi_i + Bu_{c_i}.\end{aligned} \quad (38)$$

And, based on (38), the resulting collision-free estimator dynamics is

$$\dot{\hat{\xi}}_i = \begin{cases} h_i - \frac{\nabla\phi_i\nabla\phi_i^T}{\|\nabla\phi_i\|^2}\phi_i h_i & \text{, if } \hat{\xi}_i \in \Phi_i^j - \bar{\Phi}_i^j \\ h_i & \text{, otherwise}\end{cases} \quad (39)$$

Here,

$$h_i = \bar{A}_i\hat{\xi}_i + Bu_{c_i} + LC(\hat{\xi}_i - \xi_i), \quad (40)$$

and $\{\phi_i, \Phi_i^j, \bar{\Phi}_i^j\}$ are the convex constraint variables discussed in Section III. The estimator error is the vector $e_i = \hat{\xi}_i - \xi_i$, with the dynamics

$$\dot{e}_i = \underbrace{\mathbf{Proj}(\hat{\xi}_i, h_i) - h_i}_{\text{Projection Dynamics}} + \underbrace{(\bar{A}_i + LC)e_i}_{\text{Standard Estimator}}. \quad (41)$$

Let $V_1(e_i)$, defined by

$$\lambda_{\min}(\Gamma)\|e_i\|^2 \leq V_1(e_i) = \frac{1}{2}e_i^T\Gamma e_i \leq \lambda_{\max}(\Gamma)\|e_i\|^2, \quad (42)$$

be the positive definite and decresent Lyapunov energy function associated with the estimator error dynamics. The linear closed-loop error dynamics, $\bar{A}_i + LC$, is exponentially stable, therefore, there exists a positive definite matrix Q_e, so that

$$\bar{A}_i^T\Gamma + \Gamma\bar{A}_i = -Q_e, \quad (43)$$

and, using the projection Lemma 3.1, we have

$$\Rightarrow \dot{V}_1(e_i) \leq -\frac{1}{2}\lambda_{\min}(Q_e)\|e_i\|^2. \quad (44)$$

Substituting for u_{c_i} in (38), yields

$$\begin{aligned}\dot{\xi}_i &= \bar{A}_i\xi_i + \alpha_i BG_eCe_i + BG_fC\hat{\xi}_i\\ &= (\bar{A}_i + BG_fC)\xi_i + B\underbrace{(\alpha_iG_e + G_f)}_{=\Delta G_e(\alpha_i)}Ce_i.\end{aligned} \quad (45)$$

Let $V_2(\xi_i)$, defined by

$$\lambda_{\min}(P)\|\xi_i\|^2 \leq V_2(\xi_i) = \frac{1}{2}\xi_i^TP\xi_i \leq \lambda_{\max}(P)\|\xi_i\|^2, \quad (46)$$

be the positive definite and decresent Lyapunov energy function associated with the relative error trajectory ξ_i. Taking the time derivative of $V_2(\xi_i)$, we have

$$\begin{aligned}\dot{V}_2(\xi_i) &= \xi_i^TP\dot{\xi}_i\\ &= \xi_i^TP\left[(\bar{A}_i + BG_fC)\xi_i + B\Delta G_e(\alpha_i)Ce_i\right]\\ \Rightarrow \dot{V}_2(\xi_i) &= \xi_i^TP(\bar{A}_i + BG_fC)\xi_i + \xi_i^TPB(\Delta G_eC)e_i.\end{aligned} \quad (47)$$

The gains G_i and G_f, are such that, the matrix $(\bar{A}_i + BG_fC)$ is Hurwitz. Therefore, there exists a postive definite matrix, Q_ξ, so that

$$(\bar{A}_i + BG_fC)^TP + P(\bar{A}_i + BG_fC) = -Q_\xi, \text{ and} \quad (48)$$

$$\dot{V}_2(\xi_i) \leq -\frac{1}{2}\lambda_{\min}(Q_\xi)\|\xi_i\|^2 + |(\Delta G_eCe_i, (PB)^T\xi_i)|. \quad (49)$$

Applying the Cauchy-Schwarz (C-S) inequality to $|(\Delta G_eCe_i, (PB)^T\xi_i)|$, we have

$$\dot{V}_2(\xi_i) \leq -\frac{1}{2}\lambda_{\min}(Q_\xi)\|\xi_i\|^2 + \|\Delta G_eCe_i\|\,\|(PB)^T\xi_i\|. \quad (50)$$

Using $PB = C^T$ ($\because$ the agent is ASD[15]), and substituting for ΔG_e, results in

$$\begin{aligned}\dot{V}_2(\xi_i) \leq &-\frac{1}{2}\lambda_{\min}(Q_\xi)\|\xi_i\|^2\\ &+ \left(\alpha_i\|G_e\| + \|G_f\|\right)\|C\|^2\|e_i\|\,\|\xi_i\|.\end{aligned} \quad (51)$$

Let $V(e_i, \xi_i)$, defined by

$$V(e_i, \xi_i) = V_1(e_i) + V_2(\xi_i), \tag{52}$$

be the Lyapunov energy function associated with the combined dynamics of the relative error vector, ξ_i, and the estimator error vector e_i. Its time derivative is

$$\dot{V}(e_i, \xi_i) = \dot{V}_1(e_i) + \dot{V}_2(\xi_i) \tag{53}$$

$$\begin{aligned} &\leq -\frac{1}{2}\lambda_{\min}(Q_e)\|e_i\|^2 - \frac{1}{2}\lambda_{\min}(Q_\xi)\|\xi_i\|^2 \\ &\qquad + \left(\alpha_i\|G_e\| + \|G_f\|\right)\|C\|^2\|e_i\|\,\|\xi_i\|. \end{aligned} \tag{54}$$

Here, let $\gamma_1^2 = \lambda_{\min}(Q_e)$, and $\gamma_2^2 = \lambda_{\min}(Q_\xi)$, such that

$$\begin{aligned} (\gamma_1\|e_i\| - \gamma_2\|\xi_i\|)^2 = \gamma_1^2\|e_i\|^2 + \gamma_2^2\|\xi_i\|^2 \\ -2\gamma_1\gamma_2\|e_i\|\,\|\xi_i\|. \end{aligned} \tag{55}$$

Therefore,

$$\begin{aligned} \dot{V}(e_i, \xi_i) \leq -\frac{1}{2}\big(&\gamma_1^2\|e_i\|^2 + \gamma_2\|\xi_i\|^2 \\ &- 2\left(\alpha_i\|G_e\| + \|G_f\|\right)\|C\|^2\|e_i\|\,\|\xi_i\|\big). \end{aligned} \tag{56}$$

Since,

$$\alpha_i = \frac{\sqrt{\lambda_{\min}(Q_e)}\sqrt{\lambda_{\min}(Q_\xi)}}{\|G_e\|\,\|C\|^2} - \frac{\|G_f\|}{\|G_e\|}, \tag{57}$$

$$\left(\alpha_i\|G_e\| + \|G_f\|\right)\|C\|^2 = \gamma_1\gamma_2. \tag{58}$$

Hence, $\dot{V}(e_i, \xi_i)$ reduces to

$$\dot{V} \leq -\frac{1}{2}\left(\gamma_1^2\|e_i\|^2 + \gamma_2^2\|\xi_i\|^2 - 2\gamma_1\gamma_2\|e_i\|\,\|\xi_i\|\right) \tag{59}$$

$$\text{or, } \dot{V} \leq (\gamma_1\|e_i\| - \gamma_2\|\xi_i\|)^2. \tag{60}$$

Therefore, the trajectories $e_i(t)$, and $\xi_i(t)$, are bounded. And, by Barbalat's lemma, the real valued function

$$W(e_i, \xi_i) = (\gamma_1\|e_i\| - \gamma_2\|\xi_i\|)^2 \to 0, \tag{61}$$

as $t \to \infty$. To show that the individual vectors $e_i(t)$, and $\xi_i(t)$, are asymptotically stable, consider

$$\dot{V}_1(e_i) \leq -\frac{1}{2}\lambda_{\min}(Q_e)\|e_i\|^2 \leq -\underbrace{\frac{\lambda_{\min}(Q_e)}{2\lambda_{\max}(\Gamma)}}_{=\mu} V_1(e_i), \tag{62}$$

which,

$$\Rightarrow \dot{V}_1(e_i) + \mu V_1(e_i) \leq 0. \tag{63}$$

Integrating (63) with respect to τ using the integrating factor $e^{\mu t}$, we have

$$V_1(e_i) \leq e^{-\mu\tau} V_1(0). \tag{64}$$

Further, $V_1(0) \leq \lambda_{\max}(\Gamma)\|e_i(0)\|^2$, and $\lambda_{\min}(\Gamma)\|e_i\|^2 \leq V_1(e_i)$, by which

$$\Rightarrow \|e_i(\tau)\| \leq \sqrt{\frac{\lambda_{\max}(\Gamma)}{\lambda_{\min}(\Gamma)}} e^{-\frac{\mu}{2}\tau}\|e_i(0)\|. \tag{65}$$

Therefore, $e_i(\tau) \to 0$, as $\tau \to \infty$, exponentially at the rate $\mu/2$. Next, consider

$$\begin{aligned} 0 \leq |\,\gamma_2\|\xi_i\|\,| &= |\gamma_2\|\xi_i\| - \gamma_1\|e_i\| + \gamma_1\|e_i\|\,| && (66)\\ &\leq |\gamma_2\|\xi_i\| - \gamma_1\|e_i\|\,| + |\gamma_1\|e_i\|\,| && (67)\\ &= W^{1/2}(e_i, \xi_i) + |\gamma_1\|e_i\|\,|. && (68) \end{aligned}$$

From (61), $W(e_i, \xi_i) \to 0$, as $t \to \infty$

$$\Rightarrow W^{1/2}(e_i, \xi_i) \to 0, \text{ as } t \to \infty, \tag{69}$$

Hence,

$$0 \leq \lim_{t\to\infty} |\gamma_2\|\xi_i\|\,| \leq \lim_{t\to\infty} W^{1/2}(e_i, \xi_i) + \lim_{t\to\infty} |\gamma_1\|e_i\|\,| \tag{70}$$

From (65), and (69),

$$0 \leq \lim_{t\to\infty} |\gamma_2\|\xi_i\|\,| \leq 0, \tag{71}$$

Consequently, $\xi_i(t) \to 0$, as $t \to \infty$. ■

V. Simulation Result / Illustrative Example

The purpose of this illustrative example is to verify that the numerical simulations are consistent with the theoretical predictions discussed in Sections II-IV. The formation under consideration is two dimensional and consists of nine linear agents with the 2-dimensional double integrator dynamics

$$\ddot{x} = u_x; \quad \ddot{y} = u_y. \tag{72a}$$

All the agents in the formation, except the leader (agent 1), have identical control policy, as shown in (36). The dynamic model for all the inter-agent spacing, d_i^j, is a (see (4)) step generator with the matrix $F = 0$. We choose the following output and the baseline controller gain matrices:

$$C = \begin{pmatrix} 1 & 0 & 0.125 & 0 \\ 0 & 1 & 0 & 0.125 \end{pmatrix} \text{ and } G_i = \begin{pmatrix} -0.9 & 0 \\ 0 & -0.9 \end{pmatrix},$$

which results in a stable closed-loop matrix $A + BG_iC$ for the baseline formation controller. Since the dynamic model for d_i^j is a step generator, the gain matrix G_d reduces to zero. The stable tracking controller gains are

$$G_e = \begin{pmatrix} 2.8 & 0.0 \\ 0.0 & 2.8 \end{pmatrix} \text{ and } G_f = \begin{pmatrix} 3.7 & 0.0 \\ 0.0 & 3.7 \end{pmatrix}.$$

Fig. 1 shows the agents' geometric arrangement. As mentioned in [5], the node augmentation approach was used to generate a structurally stable interaction topology. The transient instability mitigation was assessed using two simulation runs: In the first simulation run, the formation used only the baseline controller for spatial distance maintenance. In the second simulation run, the formation used the baseline controller and the projection estimator reference model and the corresponding tracking controller. In both the simulation runs, an initial command of a 90 degrees of rotation followed by 25% size reduction command was issued at time events t=1s and t=7s, respectively. Also, for both the simulation runs, the RK45 explicit solver from Python's SciPy library was used to propagate all the agent and controller states. Fig. 8 and Fig. 9 show the simulation's outcome of the first and second simulation runs respectively. Clearly, from Fig. 9, it is evident that the controller, as shown in Fig. 1, effectively avoids inter-agent collision while simulataneously satisfying asymptotic stability, and thereby mitigating transient instability.

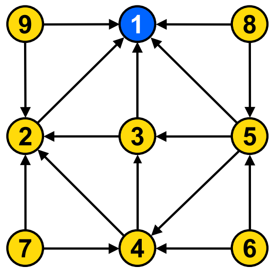

Fig. 7. Simulation formation topology.

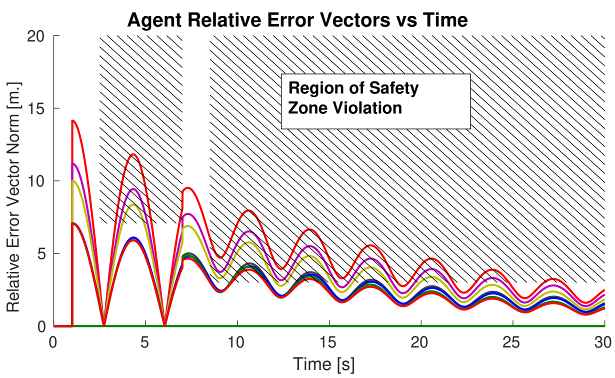

Fig. 8. Simulation 1: all agents have only the baseline controller enabled; formation reconfiguration events leads to safety-zone violations, and therefore, inter-agent collisions.

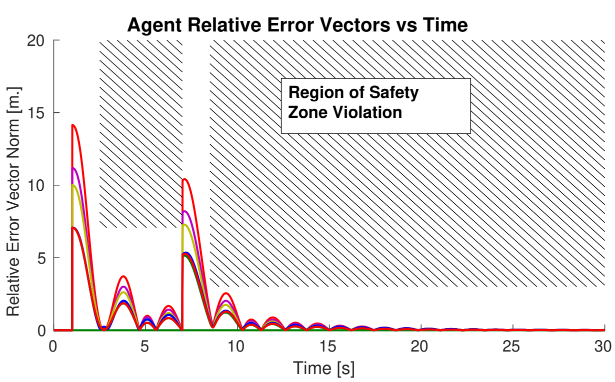

Fig. 9. Simulation 2: the baseline controller, the projection-based collision estimator, and tracking controller are enabled for all the agents; none of the agents violate the prescribed safety zone; no inter-agent collisions occur.

VI. CONCLUSIONS

This paper has proposed a novel control approach to mitigate transient stability in general N agent formation of autonomous agents that is fast and easy to implement. The formation dynamics assumed inter-agent communication availability at the outset, which eliminated the agent-to-agent interaction graph's influence on the overall dynamics. Following this, we defined the constrains and the projection operator to generate collision-free estimates of the relative error trajectories. Finally, this paper's main theoretical result substantiated the proposed architecture as a viable mechanism for mitigating transient instabilities in formations. In this paper, we focused entirely on deterministic agents, and the problem of transient instability was restricted to formation reconfiguration. The sequel to this paper and future work includes exploring and developing mitigation strategies for transient instabilities that result from external deterministic and stochastic disturbances and nonlinear effects.

ACKNOWLEDGMENT

Part of this research was carried out at the Jet Propulsion Laboratory, California Institute of Technology, under a contract with the National Aeronautics and Space Administration. ©2020 California Institute of Technology. Government sponsorship acknowledged.

REFERENCES

[1] V. P. Gehlot, M. J. Balas, and S. Bandyopadhyay, "Dynamic stability and adaptive control of networked evolving formations with weak nonlinearities," in *AIAA Scitech Forum*. AIAA, 2020.

[2] J. A. Fax and R. M. Murray, "Graph laplacians and stabilization of vehicle formations," *IFAC Proceedings Volumes*, vol. 35, no. 1, pp. 55 – 60, 2002, 15th IFAC World Congress.

[3] R. Olfati-Saber and R. M. Murray, "Consensus problems in networks of agents with switching topology and time-delays," *IEEE Transactions On Automatic Control*, vol. 49, no. 9, September 2004.

[4] L. Peppard, "String stability of relative-motion pid vehicle control systems," *IEEE Transactions on Automatic Control*, vol. 19, no. 5, pp. 579–581, 1974.

[5] R. Olfati-Saber and R. M. Murray, "Distributed structural stabilization and tracking for formations of dynamic multi-agents," in *Proceedings of the 41st IEEE Conference on Decision and Control, 2002.*, vol. 1, 2002, pp. 209–215 vol.1.

[6] A. D. Ames, J. W. Grizzle, and P. Tabuada, "Control barrier function based quadratic programs with application to adaptive cruise control," in *53rd IEEE Conference on Decision and Control*, 12 2014, pp. 6271–6278.

[7] F. Rossi, S. Bandyopadhyay, M. Wolf, and M. Pavone, "Review of multi-agent algorithms for collective behavior: a structural taxonomy," *IFAC-PapersOnLine*, vol. 51, no. 12, pp. 112 – 117, 2018, iFAC Workshop on Networked & Autonomous Air & Space Systems NAASS 2018.

[8] J. T.-Y. Wen and M. J. Balas, "Robust adaptive control in hilbert space," *Journal of Mathematical Analysis and Applications*, vol. 143, no. 1, pp. 1 – 26, 1989.

[9] H. KIMURA, "On pole assignment by output feedback," *International Journal of Control*, vol. 28, no. 1, pp. 11–22, 1978.

[10] D. Zhou, Z. Wang, S. Bandyopadhyay, and M. Schwager, "Fast, online collision avoidance for dynamic vehicles using buffered voronoi cells," *IEEE Robotics and Automation Letters*, vol. 2, no. 2, pp. 1047–1054, 2017.

[11] E. Lavretsky and K. Wise, *Robust and Adaptive Control: With Aerospace Applications*, ser. Advanced Textbooks in Control and Signal Processing. Springer London, 2012.

[12] G. Kreisselmeier and K. Narendra, "Stable model reference adaptive control in the presence of bounded disturbances," *IEEE Transactions on Automatic Control*, vol. 27, no. 6, pp. 1169–1175, 1982.

[13] P. A. Ioannou and J. Sun, *Robust Adaptive Control*. Mineola, New York: Dover Publication, Inc., 2012, p. 586.

[14] N. Hovakimyan and C. Cao, *L1 Adaptive Control Theory: Guaranteed Robustness with Fast Adaptation*, ser. Advances in Design and Control. Society for Industrial and Applied Mathematics, 2010.